LLNL'S REGIONAL MODEL CALIBRATION AND BODY-WAVE DISCRIMINATION RESEARCH IN THE FORMER SOVIET UNION USING PEACEFUL NUCLEAR EXPLOSIONS (PNEs)

Joydeep Bhattacharyya, Arthur Rodgers, Jennifer Swenson, Craig Schultz, William Walter
Lawrence Livermore National Laboratory

Walter Mooney and Geoff Clitheroe
United States Geological Survey

Sponsored by U.S. Department of Energy
Office of Nonproliferation Research and Engineering
Office of Defense Nuclear Nonproliferation
National Nuclear Security Administration

Contract No. W-7405-ENG-48

ABSTRACT

Long-range seismic profiles from Peaceful Nuclear Explosions (PNE) in the Former Soviet Union (FSU) provide a unique data set to investigate several important issues in regional Comprehensive Nuclear-Test-Ban Treaty (CTBT) monitoring. The recording station spacing (~ 15 km) allows for extremely dense sampling of the propagation from the source to ≥ 3300 km. This allows us to analyze the waveforms at local, near- and far-regional and teleseismic distances. These data are used to: 1) study the evolution of regional phases and phase amplitude ratios along the profile; 2) infer one-dimensional velocity structure along the profile; and 3) evaluate the spatial correlation of regional and teleseismic travel times and regional phase amplitude ratios. We analyzed waveform data from four PNE's (m_b = 5.1 – 5.6) recorded along profile KRATON, which is an east-west trending profile located in northern Siberia.

Short-period regional discriminants, such as P/S amplitude ratios, will be essential for seismic monitoring of the Comprehensive Nuclear-Test-Ban Treaty (CTBT) at small magnitudes (m_b<4.0). However, P/S amplitude ratios in the short-period band, 0.5 – 5.0 Hz, show some scatter. This scatter is primarily due to propagation and site effects, which arise from variability in the elastic and anelastic structure of the crustal waveguide. Preliminary results show that Pg and Lg propagate efficiently in north Siberia at regional distances. The amplitude ratios show some variability between adjacent stations that are modeled by simple distance trends. The effect of topography, sediment and crustal thickness, and upper mantle discontinuities on these ratios, after removal of the distance trends, will be investigated.

The travel times of the body wave phases recorded on KRATON have been used to compute the one-dimensional structure of the crust and upper mantle in this region. The path-averaged one-dimensional velocity model was computed by minimizing the first arriving P-phase travel-time residuals for all distances (Δ = 300 – 2300 km). A grid search approach was used in the minimization. The most significant features of this model are the negative lid-gradient and a low-velocity zone in the upper mantle between the depths of 100 – 200 km; precise location of the LVZ is poorly constrained by the travel time data. We will extend our investigation to additional PNE lines to further investigate the amplitude and travel-time variations in eastern and central Eurasia.

Finally, the dense station spacing of the PNE profiles allows us to model the spatial correlation of travel times and amplitude ratios through variogram modeling. The statistical analysis suggests that the correlation lengths of the travel-time and amplitude measurements are 12° and 8°, respectively.

This work was performed under the auspices of the U.S. Department of Energy by University of California Lawrence Livermore National Laboratory, under contract No. W-7405-Eng-48. LLNL contribution number UCRL-JC-138991.

Key words: PNE, Former Soviet Union, Seismic Calibration

OBJECTIVE

Peaceful nuclear explosions (PNEs) conducted by the Former Soviet Union (FSU) provide a unique data set to investigate the propagation of high-frequency regional phases for Comprehensive Nuclear-Test-Ban Treaty (CTBT) monitoring. This paper presents our initial results in calibrating the aseismic eastern FSU using PNEs. The PNE data are part of the large dataset of dense, linear, long-range, three-component (at two different instrument gains) profiles recorded by Russian scientists between 1965 - 1988. This dataset gives us a unique tool with which to probe the crust and mantle structure in Northern Eurasia and investigate regional phase phenomenology. In this paper, we will document our analysis in extracting and archiving the KRATON profile in northern Siberia. This dataset consists of waveforms at local, near- and far-regional, and upper mantle distances at nominal station spacing of about 15 km. Travel times of first arriving P-waves are used to develop one-dimensional models. Residuals relative to these models are characterized by their spatial correlation functions (variograms), which is an essential element of travel-time correction surface development using the Bayesian kriging method (*Schultz et al.* 1998). Ratios of high-frequency (0.5-10 Hz) regional phase amplitudes are widely viewed as important seismic discriminants. The distance and path dependence of regional phase amplitudes and amplitude ratios varies regionally because of variations in elastic and anelastic structure of the earth. The scatter introduced by distance and path effects can inhibit identification of explosions from natural seismicity. We employed the dense sampling of the PNE data to investigate the distance and path dependence of regional phase amplitudes. Additionally, the spatial correlation structure of the travel-time and amplitude ratio data is investigated using PNE data sets. Finally, the lateral variations of travel-time residuals, with respect to standard global model *AK135*, and amplitude ratios have been compared to variations of Moho and basement thickness.

RESEARCH ACCOMPLISHED

Introduction

Central and Eastern FSU is largely aseismic; therefore, it is impossible to calibrate these regions with earthquake data. For instance, it is difficult to use natural seismicity, a dataset widely used in most other parts of the world, to estimate these seismic properties. Fortunately, active source seismic data recorded in this region can be used for calibration purposes. During the period extending from January 1965 to September 1988, Russian scientists carried out dense seismic recordings of 122 PNEs. These explosions were carried out at several distinct geological settings and were widely dispersed within the Former Soviet Union (*Sultanov et al.* 1999). At LLNL, we have archived a subset of these PNEs.; namely, data from the profiles QUARTZ, KRATON, KIMBERLITE, METEORITE, and RIFT, which traverse regions of Central and Eastern FSU, are available to us (Figure 1). In total, we have data from 25 PNEs in our database. These profiles cross several different tectonic regions, including the East European Platform, Ural Mountains, West Siberian Platform, Siberian Craton, Altay – Sayan Fold Belt, and the Baikal Rift region. Two of the salient features of the PNE dataset are the closely spaced stations, between 10 – 20 km, and coverage of a wide range of source-to-receiver distances (from near-source to greater than 30°), which allows us to model the propagation and evolution of seismic phases with an extremely high resolution.

Dataset

In this paper, we present our analysis using the data from the KRATON line (Figure 1). This is an east-west trending profile that crosses, for the major part of its length, the Angara Archean craton, the basement core of the East Siberian platform. A significant portion of this profile also crosses the West Siberian Platform, which lies between the Uralides and the Angara craton. The western-most PNE lies on the western edge of the West Siberian basin. The data were digitized from analogue recordings in a 0.5- to 20-Hz band (*Solodilov* 1997). The usable frequency range for the KRATON data is about 0.5 – 10 Hz, though the signal above 5 Hz is low. So, our analysis is carried out in the 0.5- to 5.0-Hz band. For each station, we have three component recordings: vertical, radial and transverse. For each of these components, there are low- and high-gain channels. Since the high-gain channels are frequently clipped, most of the analysis is carried out using the low gain channel. The signal-to-noise ratio of the first arrival is good (*Mechie et al.* 1997); hence, its travel time can be robustly determined. In addition, several regional phases are clearly observed. Teleseismic Pn is clearly observed at distances up to 2000 km. The Pg phase efficiently propagates up to 1500 km. Importantly, we observe a significant difference in the moveout velocities of both Lg and Sn as well as the variation of Lg amplitude laterally. As reported in *Nielsen et al.* (1999), there is a significant scattered ("coda") energy at distances between 1000 – 1500 km.

There were four PNE shots along the KRATON profile, named KRATON1 – KRATON4. The magnitudes for these shots are 5.5, 5.2, 5.1 and 5.6 respectively, and had burial depths between 567 – 886 meters (*Sultanov et al.* 1999). In this paper, we show the results from the KRATON3 shot as the results are similar for the other shots.

Travel-Time Modeling

For each PNE, we have picked the travel times of first arriving *P* wave. Figure 2 shows the residuals of these picks as a function of source-receiver distance. The residuals are computed with respect to the predictions of a standard global model, *AK135* (*Kennett et al.* 1995). As we observe in Figure 2, there is a significant distance-dependent trend in the residuals indicating that *AK135* is inadequate for this region. We estimated a 1-dimensional model for the line. To avoid complications from Pg - Pn crossover in the travel-time curve, we limit our analysis to stations with source-receiver distances being greater than 300 km. The longest source-receiver distance considered for KRATON3 is 2301 km. A grid search algorithm is adopted to identify the model that fits the data the best. The grid-search is carried out in two ways: by varying the crustal structure and by varying the mantle structure. In the former case, modeling technique is similar to that of *Swenson et al.* (2000). Simple crust and upper mantle velocity models are generated by varying the crustal thickness (30 – 55 km), upper crustal Vp (5.5 – 7.0 km/s), lower crustal Vp (6.6 – 8.0 km/s) and the upper mantle Vp (7.9 – 8.1 km/s). The parameters that remain constant are the sediment thickness (= 4 km), sediment Vp (=4 km/s), thickness of the mantle lid (= 25 km) and the P-wave mantle velocity in the mantle lid. The mantle structure is similar to *AK135* below the 410-km discontinuity. A linear gradient, joining the lid velocity to the velocity at 410 km, is used for the rest of the upper mantle. We calculate travel times through each regionalized *P*-wave velocity model using the single-valued *tau-p* formulation similar to that of *Buland and Chapman* (1983) to produce standard travel-time tables. The tables are populated with travel times, parameterized by distance and depth, and a root-mean-square (rms) measure of misfit is adopted. Since the travel-time modeling process is non-linear and the number of model parameters limited, the solution is non-unique. In practice, we have a suite of models that can fit the data equally well. To avoid this ambiguity, we adopt the following procedure. We rank the models based on the rms misfit with the data and select the top 10% of the models; these models fit the data nearly equally well. We then compare these models to the global average model *AK135* and select the model that is closest to *AK135* in shape. In the second-grid search, we keep a uniform crustal velocity but vary its thickness. We allow for more complicated mantle models with changes in the velocity gradient above the transition zone. This allows us to explore the possibility of low-velocity zones (LVZ) in the upper mantle.

We obtain significantly better fits when we allow the mantle structure to deviate away from *AK135*. We show the best fitting one-dimensional velocity model for KRATON3 in Figure 3. Note that we have combined the measurements from both move-out directions (East and West). We plotted the velocity structure of *AK135* for reference. It is clear from Figure 3 that both the crust and uppermost mantle velocities, on average, are faster along KRATON3 compared to the global average. This result is expected in Siberia, which is underlain by Archean crust to the west and Proterozoic crust to the east. The faster velocities are primarily an expression of a stable crustal structure. High-resolution global models have also shown high velocities in the upper mantle going to depths of up to 450 km (*Masters, et al.* (1999).

The travel-time modeling technique described above is adequate for the analysis of data with a global distribution of stations and events where the source-receiver paths encounter a wide range of geological settings. To be consistent in modeling these paths with the same set of models, it is useful to limit the range of possible models. On the other hand, when we have a regional distribution of stations and sources, we can allow ourselves to search over a different set of models that are more appropriate for that region. This is particularly true for KRATON where previous studies by *Solodilov* (1997) and *Nielsen, et al.* (1999) have shown significant low-velocity zones and variations in mantle velocity gradients, respectively. To account for these structures, we now search over models where the mantle velocity gradient is allowed to vary between –0.002 and 0.002. We find that the best models from this set have significantly better fits, i.e., the rms difference between the data and the model predictions is decreased by as much as 40 %. The best fitting model is shown in Figure 3. The most significant feature of this model is the presence of a LVZ in the upper mantle at a depth of 150 – 200 km, similar to the results of *Nielsen, et al.* (1999). Importantly, this model indicates a negative mantle-lid gradient. Figure 4a shows the spatial variation of the travel-time residuals for the best fitting model. We show the topography as a proxy for tectonics. We observe that, though there is no obvious correlation of travel-time variations with station location, we see that in general Western Siberia has negative

residuals compared to Eastern Siberia. This difference might be due to the faster mantle in the west or to the thicker crust observed in Eastern Siberia.

The variance structure of the travel-time picks can give us important insights into the correlation length of regional structures along with robust estimates of measurement errors *Myers and Schultz* (2000). We first compute the mean square differences of all pairs of observations (travel times) as a function of inter-pair distance, i.e., a variogram. We then model this variogram using three statistical parameters: (1) correlation length (range) representing the spatial variability; (2) the background variance (σ_B), representing the overall variability of the data; and (3) the measurement error (σ_M). The measurement error is simply the variance of collocated data, which is the variogram at zero lag. Unlike *Myers and Schultz* (2000), we carry out a shot-specific travel-time analysis. Thus, we will model the variograms for each shot separately. We show the variogram for KRATON3 in Figure 4b where we chose to bin the squared differences in 1° bins. The measurement error for the dataset is 0.06 s, which is low as the source is a single nuclear explosion with well-known location and origin time. The correlation length for KRATON3 is 12° and represents the range at which the data are uncorrelated.

Regional Phase Amplitudes

The amplitudes of regional phases (Pn, Pg, Sn and Lg) in the frequency range 0.5-10 Hz are widely recognized as effective discriminants for distinguishing explosions from natural earthquakes (*Taylor et al,* 1988; *Walter et al,* 1995; *Hartse et al,* 1997). Ratios of regional P- and S-wave phases display distance trends because of differential attenuation and geometric spreading. However, in addition to distance effects, the amplitudes of these phases can vary greatly because of lateral variations in crustal and uppermost mantle structure (both elastic and anelastic). This variability is referred to as path effects. Site effects due to local geology at the recording site can lead to additional variability. After the distance trend is removed, substantial scatter can remain in the ratios because of path effects.

We measured the amplitude ratios Pg/Lg, Pn/Lg and Pn/Sn using the KRATON PNE shots. Amplitude measurements were made in the time domain filtering the traces, windowing the phases and computing the rms amplitude. Individual phases were isolated with group velocity windows (Pn 8.3-7.6 km/s; Pg 6.8-5.8 km/s; Sn 4.6-4.0 km/s & Lg 3.6-3.0 km/s). Problems associated with digitization and band-limited instrument response restrict the usable frequency content of the data. Thus, we simply measured the rms amplitude of each phase in the band 0.5-5 Hz. This is a fairly broad bandwidth. We will investigate if narrower frequency bands can be used with these data.

Figure 5 shows the Pg/Lg, Pn/Lg and Pn/Sn amplitude ratios (0.5-5 Hz) versus distance for the KRATON 3 shot. Linear regression fits to the $\log_{10}$ ratios are plotted along with 1-σ uncertainties. The data are well modeled by the linear trend; however, deviations are apparent. In particular, ratios for the eastern and western stations (relative to the shot location) show different behavior in Figure 5. This behavior reveals that path and site effects impact the observed P/S ratios.

Much effort has been focused on modeling the path effects on regional phases (e.g., *Fan and Lay* 1998; *Rodgers et al, 1*999; *Phillips* 1999). It is now well established that correction surfaces produced by Bayesian kriging (*Schultz et al,* 1998) is the optimal method for representing path effects on regional phases (*Rodgers et al,* 1999; *Phillips* 1999). In order to perform the kriging calculations, it is necessary to characterize the statistical properties and spatial correlation of the data by modeling the variogram. Figure 6 shows a map of the Pg/Lg amplitude ratios of the KRATON 3 shot and the associated variogram. The distance trend of the Pg/Lg ratios was removed revealing the path and site effects. The variogram demonstrates that the data become more poorly correlated as the inter-pair distance increases. We modeled the variogram with a monotonically increasing function that asymptotically approaches the sum of measurement and background variances (Figure 6b). The range (8.4º) governs the rise of the function and represents the range at which the data become uncorrelated. This characteristic range is typical of other regions we have studied (*Rodgers et al,* 1999). The measurement uncertainty (σ_M) is low because the source is a single nuclear explosion. Errors in the variogram measurements (error bars in Figure 6b) are small because the dense station spacing provides many measurement pairs at small inter-station ranges.

CONCLUSIONS AND RECOMMENDATIONS

We document our analyses of the KRATON PNE (shot 3) in northern Siberia. The 1-D travel-time modeling shows a significant low-velocity zone between 150- to 200-km depths. We are developing regionalized 1-D and 2-D travel-time correction models for this region following the technique of *Swenson et al*, (2000). The amplitude ratios show a linear trend with distance. The variogram modeling suggests that the correlation lengths for the travel times are 12° and for the amplitude ratios about 8°. In the future we will investigate the statistical properties of the travel-time and amplitude data. In particular we will consider regional sub-sets of the data and compare the correlation structure of the data in different regions. In order to improve velocity models for travel-time analysis and to understand the behavior of far-regional P, we will model the upper mantle triplication waveforms. We will also investigate the frequency dependence of regional-phase amplitude behavior and document the propagation efficiency of the regional phases as a function of frequency.

REFERENCES

Buland, R., and C. Chapman (1983), The Computation of Seismic Travel Times, *Bulletin Seismological Society of America*, *73* , 1271 - 1302.

Fan, G., and T. Lay (1998), Regionalized Versus Single-Station Waveguide Effects on Seismic Discriminants in Western China, *Bulletin of the Seismological Society of America*, ***88*** , 1260-1274.

Hartse, H., S. Taylor, S. Phillips, and G. Randall (1997), A Preliminary Study of Regional Seismic Discrimination in Central Asia with Emphasis on Western China, *Bulletin of the Seismological Society of America*, ***87***, 551-568.

Kennett, B., E. Engdahl, and R. Buland (1995), Constraints on Seismic Velocities in the Earth from Travel Times, *Geophysical Journal International*, ***122***, 108-124.

Masters G., H. Bolton, and G. Laske (1999), Joint Seismic Tomography for P and S Velocities: How Pervasive are Chemical Anomalies in the Mantle?, *EOS Trans. AGU*, ***80***, S14.

Mechie, J., A. Egorkin, L. Solodilov, K. Fuchs, F. Lorenz, and F. Wenzel (1997), Major Features of the Mantle Velocity Structure Beneath Northern Eurasia from Long-Range Seismic Recordings of Peaceful Nuclear Explosions, in *Upper Mantle Heterogeneties from Active and Passive Seismology*, edited by K. Fuchs, pp. 33 - 50, Kluwer Academic, Netherlands.

Myers, S. and C. Schultz (2000), Improving Sparse Network Seismic Location with Bayesian Kriging and Teleseismically Constrained Calibration Events, *Bulletin of the Seismological Society of America*, ***90***, 199 - 211.

Nielsen, L., H. Thybo, and L. Solodilov (1999), Seismic Tomographic Inversion of Russian PNE Data Along Profile KRATON, *Geophysical Research Letters*, ***26***, 3413 - 3416.

Phillips, W (1999), Empirical Path Correction for Regional Phase Amplitudes, *Bulletin of the Seismological Society of America*, ***89***, 384-393.

Rodgers, A., W. Walter, C. Schultz, S. Myers, and T. Lay (1999), A Comparison of Methodologies for Representing Path Effects on Regional P/S Discriminants, *Bulletin of the Seismological Society of America*, ***89***, 394-408.

Schultz, C., S. Myers, J. Hipp, and C. Young (1998), Stationary Bayesian Kriging: Application of Spatial Corrections to Improve Seismic Detection, Location and Identification, *Bulletin of the Seismological Society of America*, ***88***, 1275-1288.

Solodilov, L. (1997), The GEON Center: 25 years of Implementation of PNE in Studies of Earth's Deep Structure, in *Upper Mantle Heterogeneities from Active and Passive Seismology*, edited by K. Fuchs, pp. 1 - 10, Kluwer Academic Publishers.

Sultanov, D., J. Murphy, and K. Rubenstein (1999), A Seismic Source Summary for Soviet Peaceful Nuclear Explosions, *Bulletin of Seismological Society of America*, ***89***, 640-647.

Swenson, J., C. Schultz, W. Hanley, and S. Myers (2000), Using Radially Heterogeneous and Azimuthally Invariant Travel-Time Models to Improve Seismic Event Location in the Middle East and North Africa, UCRL-JC-135465 abs.

Taylor, S., N. Sherman, and M. Denny (1988), Spectral Discrimination Between NTS Explosions and Western United States Earthquakes at Regional Distances, *Bulletin of the Seismological Society of America*, ***78***, 1563 - 1579.

Walter, W., K. Mayeda, and H. Patton (1995), Phase and Spectral Ratio Discrimination Between NTS Earthquakes and Explosions. Part 1: Empirical Observations, *Bulletin of the Seismological Society of America*, ***85***, 1050 - 1067.

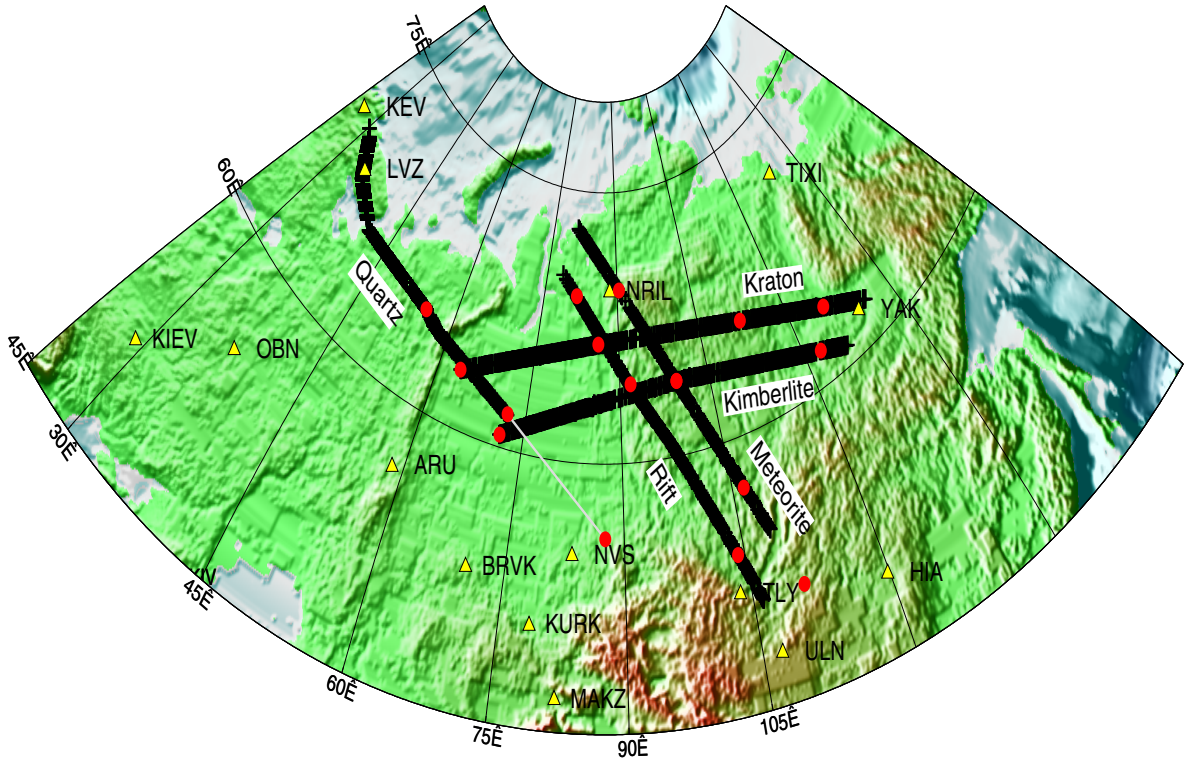

Figure 1. Soviet Peaceful Nuclear Explosion (PNE) datasets available at LLNL. Permanent three component, broadband stations in the region are also shown. The PNE shot points are shown in red circles and PNE stations are shown by +. The permanent stations are shown by the yellow triangles. The names of each PNE profile are indicated.

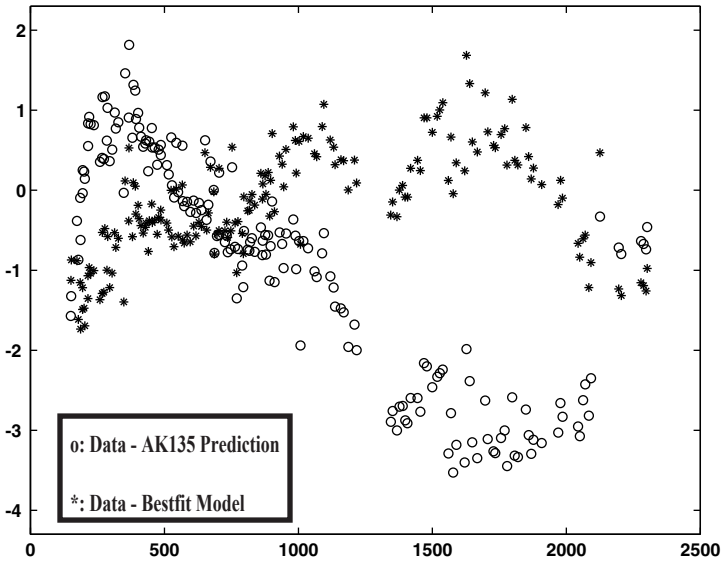

Figure 2. Travel-time residuals as a function of distance range for KRATON3. We observe a strong distance dependence for the AK135 residuals, suggesting that this model cannot adequately explain the data. The distance trends for the bestfit model is much less pronounced. We also see that the amplitude of the misfit is significantly decreased for the bestfit model.

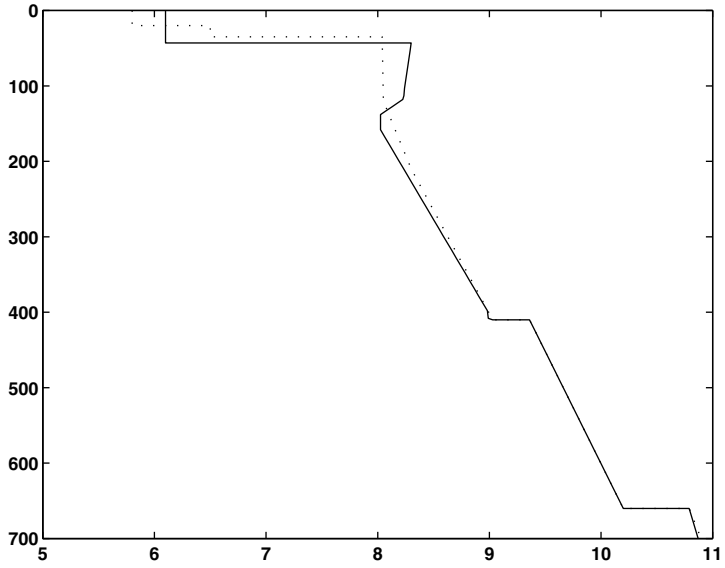

Figure 3. Bestfitting 1-dimensional model for the KRATON3 profile is shown in the solid line. The global reference model, AK135, is shown in the dotted line. The crust and the uppermost mantle is significantly faster for KRATON3 compared to the global average. We also find evidence for a significant low-velocity zone below the mantle lid at depths between 150 - 200 km. Note the negative velocity gradient in the mantle lid.

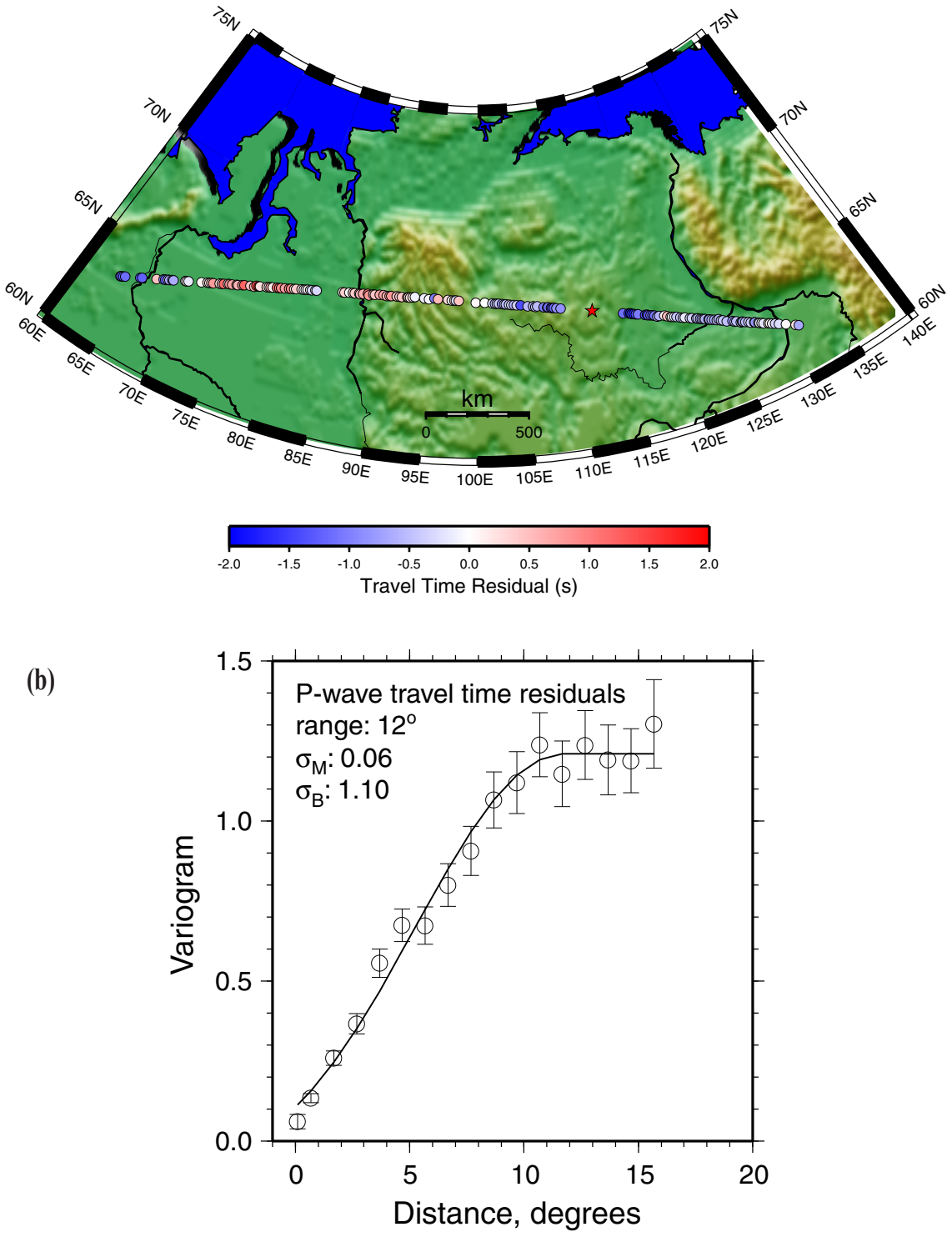

Figure 4. Spatial variation of travel-time residual for the bestfitting 1-D model for KRATON3 (Model_2 as described in text). (a) Map of residuals plotted at station locations on top of topography. Removal of the travel-time predictions of the best-fitting model largely reduces the distance trend revealing path and site effects. We observe faster (negative) residuals for the Eastern stations. (b) Variogram of the travel-time residuals along with our model. The model is parameterized by the range, the measurement error (σ_M) and the background error (σ_B). The range gives us an estimate of the correlation length for the region. The low measurement error indicates the robustness of the travel-time picks.

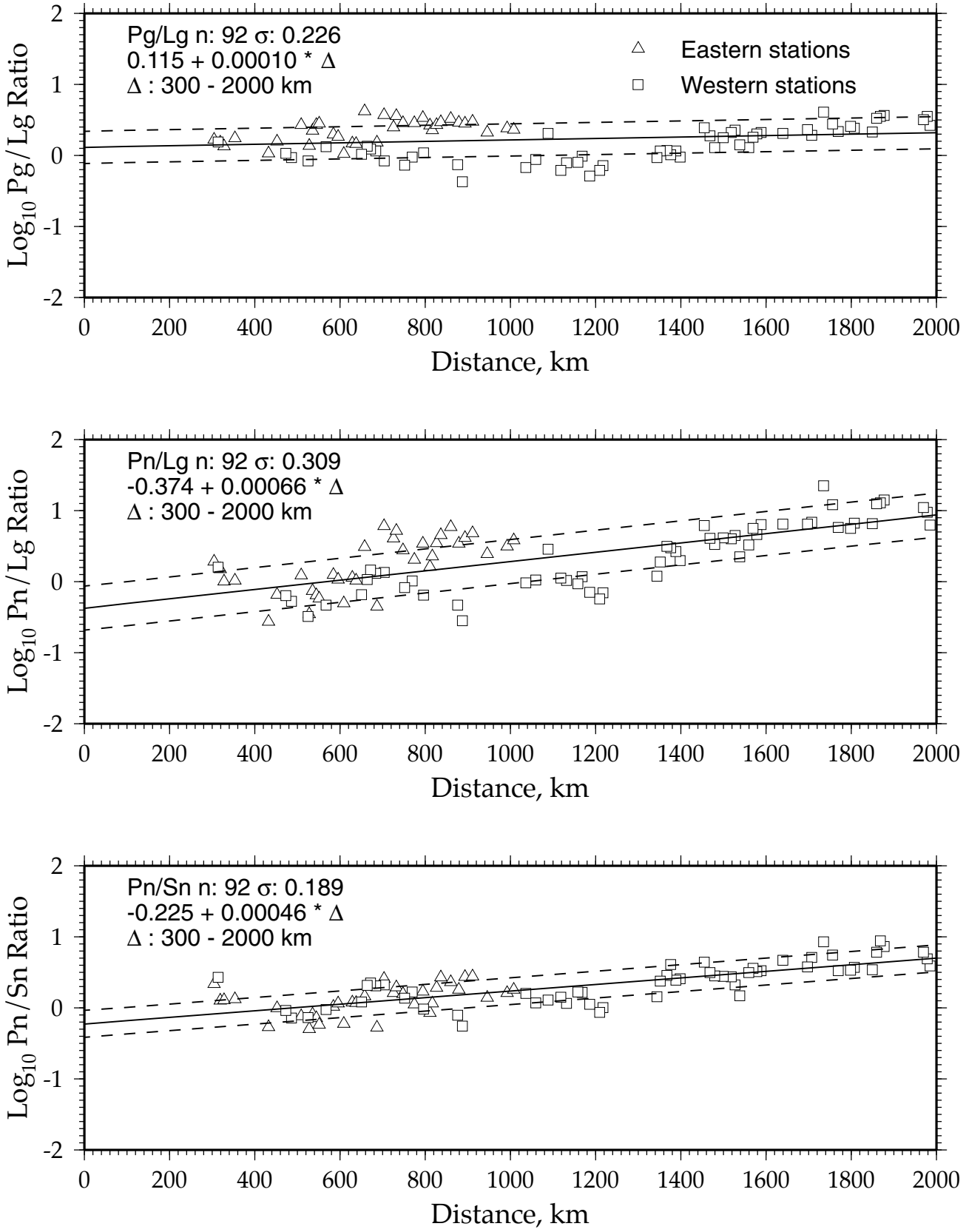

Figure 5. Distance trends of Pg/Lg (top), Pn/Lg (center) and Pn/Sn (bottom). Ratios were taken in the band 0.5-5 Hz. Linear regression fits and 1-σ uncertainties (solid and dashed lines, respectively) are shown. The ratios for eastern and western stations are plotted with triangles and squares, respectively. We considered the ratios with distances between 300-2000 km.

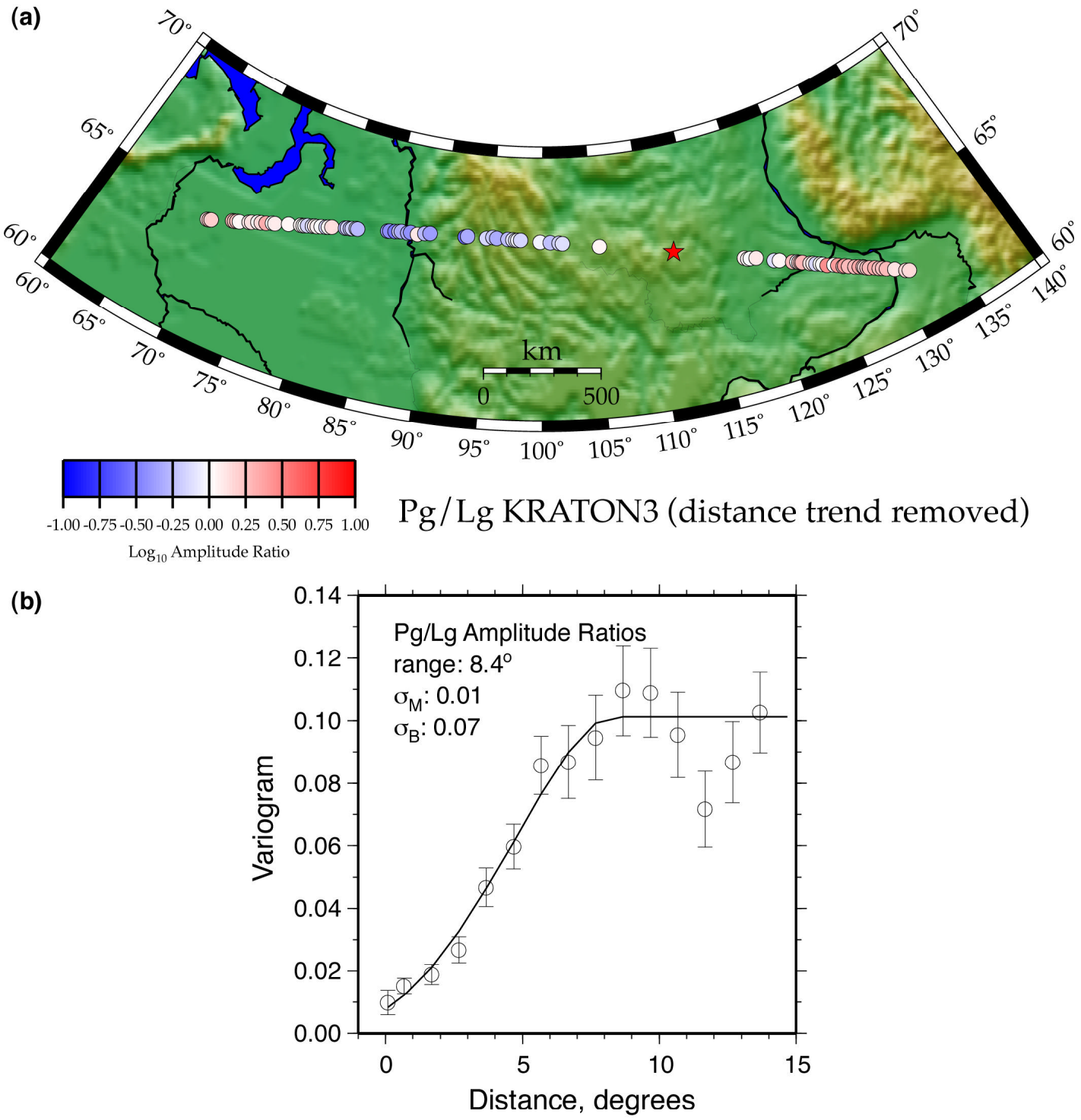

Figure 6. (a) Map of Pg/Lg ratios (0.5-5.0 Hz) for the KRATON3 PNE. Ratios are color coded according to the scale. The distance trend was removed revealing path and site effects. (b) Variogram of the Pg/Lg ratios along with our model. The model is parameterized by a range, the measurement error (σ_M) and the background error (σ_B), similar to that for the travel times.